ELSEVIER

Remote Sensing of Environment 79 (2002) 213–224

Remote Sensing of Environment

www.elsevier.com/locate/rse

A simple interpretation of the surface temperature/vegetation index space for assessment of surface moisture status

Inge Sandholt[a,*], Kjeld Rasmussen[a], Jens Andersen[b]

[a]*Institute of Geography, University of Copenhagen, Ostervoldgade 10, 1350 Copenhagen, Denmark*
[b]*Department of Hydrodynamics and Water Resources, Technical University of Denmark, 2800 Lyngby, Denmark*

Received 9 August 1999; received in revised form 6 November 2000; accepted 19 February 2001

Abstract

A simplified land surface dryness index (Temperature–Vegetation Dryness Index, TVDI) based on an empirical parameterisation of the relationship between surface temperature (T_s) and vegetation index (NDVI) is suggested. The index is related to soil moisture and, in comparison to existing interpretations of the T_s/NDVI space, the index is conceptually and computationally straightforward. It is based on satellite derived information only, and the potential for operational application of the index is therefore large. The spatial pattern and temporal evolution in TVDI has been analysed using 37 NOAA-AVHRR images from 1990 covering part of the Ferlo region of northern, semiarid Senegal in West Africa. The spatial pattern in TVDI has been compared with simulations of soil moisture from a distributed hydrological model based on the MIKE SHE code. The spatial variation in TVDI reflects the variation in moisture on a finer scale than can be derived from the hydrological model in this case.

1. Introduction

Hydrological modelling of large watersheds requires input of data for a substantial number of variables at short time intervals. Proper description of large and heterogeneous watersheds requires that models are "distributed," i.e., that the model takes into account the spatial distribution of each of the variables. Provision of data for such distributed models is particularly problematic in developing countries with little infrastructure and few resources for continuous monitoring of environmental variables. Where watersheds transcend national boundaries, these problems become even more pronounced. It is obvious that use of Earth Observation (EO) data is potentially of great interest in such contexts. Widely used distributed hydrological models, such as MIKE SHE (Refsgaard & Storm, 1995), have not been designed to use EO data as inputs, and methods for extracting hydrological information from EO data have not been developed with this particular use in mind. Thus, there is a need to develop or modify methods and algorithms for determining key parameters in distributed hydrological models from EO data, respecting the requirements on spatial and temporal resolution.

One of the EO data sources of greatest relevance at the present time is NOAA-AVHRR. It produces daily coverage with a spatial resolution corresponding well to what is required by a distributed hydrological model of a large watershed, such as the Senegal River basin studied here. Its five bands in the visible, near, shortwave, and thermal infrared parts of the electromagnetic spectrum carry information on at least three key variables in hydrological models: vegetation cover and leaf area index (LAI), albedo and evapotranspiration, or soil humidity, the later of which are both related to the observable radiative surface temperature. Other presently available satellite sensor systems, including GOES/Meteosat and SSM/I, are useful as well, e.g., for estimating rainfall (e.g., Zeng, 1999). New systems, such as SPOT Vegetation, MODIS and MERIS, and — not the least — Meteosat Second Generation, add further to the potential of EO for distributed hydrological mapping.

The present paper aims at demonstrating how NOAA-AVHRR and other similar data may be used to estimate temporal and spatial patterns of soil moisture, a key variable in distributed hydrological models. The basic approach is to interpret the so-called T_s/NDVI space in terms of surface soil moisture status. The results are compared with soil

* Corresponding author. Fax: +45-3-532-2501.
E-mail address: is@geogr.ku.dk (I. Sandholt).

0034-4257/01/$ – see front matter
PII: S0034-4257(01)00274-7

moisture derived from a hydrological model. The study area is the Senegalese part of the semiarid Sahel.

2. Background

The potential of obtaining information about the energy and water status of a surface or for classification of land cover through the relation between remotely sensed surface temperature (T_s) and vegetation index (e.g., the normalised difference index, NDVI) has been investigated by several authors (e.g., Carlson, Gillies, & Perry, 1994; Clarke, 1997; Gillies, Carlson, Gui, Kustas, & Humes, 1997; Goetz, 1997; Lambin & Ehrlich, 1996; Moran, Clarke, Inoue, & Vidal, 1994; Nemani, Pierce, Running, & Goward, 1993; Nemani & Running, 1997, 1989; Smith & Choudhury, 1991). The complementary information in the thermal and the visible/near infrared wavelengths has proven to be well suited to monitoring vegetation status and stress, specifically in relation to water stress. NDVI is a rather conservative indicator of water stress, because vegetation remains green after initial water stress. In contrast, the surface temperature can rise rapidly with water stress (e.g., Goetz, 1997). The amount of vegetation present is an important factor, however, in surface temperature estimation.

T_s and NDVI in combination can provide information on vegetation and moisture conditions at the surface. Several studies focus on the slope of the T_s/NDVI curve for this purpose (e.g., Friedl & Davis, 1994; Nemani & Running, 1989; Smith & Choudhury, 1991). The T_s/NDVI slope is related to the evapotranspiration rate of the surface, and has been used to estimate air temperature (Boegh, Soegaard, Hanan, Kabat, & Lesch, 1998; Prihodko & Goward, 1997). Analysis of the T_s/NDVI slope has also been used to assess information related to areal averaged soil moisture conditions (Goetz, 1997; Goward, Xue, & Czajkowski, 2001), Nemani and Running (1989) related the slope of the T_s/NDVI relationship to the stomatal resistance and the evapotranspiration of a deciduous forest. Their approach was later extended to use the information in the T_s/NDVI space (e.g., Moran, Clarke, Inoue, et al., 1994).

The first part of the sentence should read: "A scatterplot of remotely sensed surface temperature and a vegetation index often results in a triangular shape (Price, 1990, Carlson et al., 1994), or a trapezoid shape (Moran, Clarke, Inoue, et al., 1994) if a full range of fractional vegetation cover and soil moisture contents is represented in the data. Since different surface types may have different T_s/NDVI slope and intercept for equal atmospheric and surface moisture conditions, the choice of scale may influence the shape of the relationship.

The location of a pixel in the T_s/NDVI space is influenced by many factors, and a number of studies have been done to provide interpretations. Some of these may have had a theoretical basis (e.g., Moran et al., 1994), some relied on simulations using Soil–Vegetation–Atmosphere Transfer (SVAT) models, (Gillies et al., 1997; Moran, Clarke, Kustas, Weltz, & Amer, 1994), some have been based on in situ measurements (Friedl & Davis, 1994), while others are largely based on analyses of remotely sensed data (Clarke, 1997). A range of vegetation types and crops have been studied under a variety of climatic conditions, and the scales studied range from meters to global. It may not be surprising, therefore, that the interpretations differ widely. The approach described by Moran, Clarke, Inoue, et al. (1994) accounts for partially vegetated surfaces. They suggest a Water Deficit Index (WDI), related to the actual and potential evapotranspiration rates of a surface. Once the trapezoid defining the temperature/vegetation index was estimated using a SVAT model, WDI was estimated from remotely sensed and meteorological data, using the relationship between surface temperature minus air temperature and a vegetation index. Carlson, Gillies, & Schmugge (1995) showed, using a SVAT model, how surface soil moisture availability and fractional vegetation cover can be derived from analysis of the temperature/vegetation index space. Assuming that the vegetation index is linearly related to fractional vegetation cover, and plotting the surface temperature–air temperature gradient as a function of the vegetation index, Moran, Clarke, Kustas, et al. (1994) derived the shape of T_s/NDVI space from model simulations, and gave a theoretical justification of the concept. They suggested that the energy balance at the surface is a controlling factor, which justifies the use of the surface air temperature gradient via its relation to sensible heat flux.

Interpretation of surface temperature for sparse canopies is not straightforward because the measured temperature integrates the temperature of the soil surface as well as the temperature of the vegetation, and the components may not "mix" linearly. Other studies have shown that, at least for well-watered surfaces, the relationship between surface temperature and NDVI is more directly related to surface soil moisture, through the increase of the thermal inertia of the soil with surface soil moisture rather than as a limiting control on latent heat (Friedl & Davis, 1994).

We explored an empirical simplification of the WDI. The simplification takes into account variations in air temperature, radiation balance, and atmospheric forcing by empirical estimation of the T_s/NDVI space. The method is conceptually and computationally straightforward, and only satellite-derived information is used.

2.1. Interpretation of the T_s/NDVI space

The following mechanisms are suggested as those determining the location of a pixel in the T_s/NDVI space. The interpretation is based on findings in the literature (e.g., Carlson et al., 1994; Gillies et al., 1997; Goetz, 1997; Lambin & Ehrlich, 1996; Moran, Clarke, Inoue, et al., 1994; Nemani et al., 1993; Nemani & Running, 1997, 1989).

2.1.1. Fractional vegetation cover

The fractional vegetation cover can be related to spectral vegetation indices, through a simple, yet not necessarily linear transformation. Likewise, fractional vegetation cover influences the amount of bare soil and vegetation visible to a sensor and differences in radiative temperature between the soil and the vegetation canopy will affect the spatially integrated T_s.

2.1.2. Evapotranspiration

Evapotranspiration can largely control the surface temperature through the energy balance of the surface. The less the evapotranspiration, the more energy available for sensible heating of the surface. Stomatal resistance to transpiration is a key factor, which is partly controlled by soil moisture availability.

2.1.3. Thermal properties of the surface

Heat capacity and conductivity — and thus the thermal inertia — influence T_s in the case of partly vegetated surfaces. These thermal properties are a function of soil type, and change with surface soil moisture.

2.1.4. Net radiation

The available energy incident at the surface affects T_s. The radiative control of surface temperature implies that areas with a lower net shortwave radiation balance (e.g., due to a high albedo) will have lower temperatures, all else equal. Albedo is controlled by soil type, surface soil moisture, and vegetation cover. Incident radiation also affects the stomatal resistance to transpiration, which factors into the partitioning of net radiation into sensible and latent heat.

2.1.5. Atmospheric forcing and surface roughness

The ability to conduct heat away from the surface into the atmosphere is an important component in the control of surface temperature. This, in part, explains how vegetated surfaces with higher roughness have lower surface temperatures (all else equal) compared to bare soil and influences the shape of the T_s/NDVI space. Similarly, homogeneous surfaces with unlimited water supply (for instance, irrigated surfaces) may have higher surface temperature than expected, if heat conductivity into the atmosphere is reduced by poor mixing (Nemani & Running, 1997).

2.1.6. Interacting factors

These factors have been summarised in Fig. 1. No direct relation between surface temperature and surface soil moisture is evident, but soil moisture is clearly a critical factor in the mechanisms involved. For bare soils at constant irradiance, surface temperatures are primarily determined by soil moisture content, via evaporative control and thermal properties of the surface. Fig. 2 shows the conceptual T_s/NDVI space, with T_s plotted as a function of NDVI. The left edge represents bare soil from the range dry to wet (top–down). As the green vegetation amount increases along the *x*-axis (with NDVI), the maximum surface temperature decreases. For dry conditions, the negative relation is defined by the upper edge, which is the upper limit to surface temperature for a given surface type and climatic forcing.

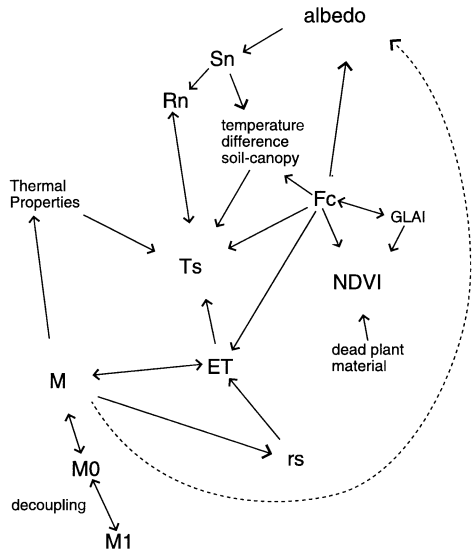

Fig. 1. Illustration of the factors determining surface brightness temperature. The circled variables can be estimated using satellite data. Sn = shortwave net radiation balance; Rn = net radiation balance; GLAI = green leaf area index; Fc = fractional vegetation cover; ET = evapotranspiration; rs = stomatal resistance; M1 = soil moisture content (root zone); M0 = top soil moisture content.

Many of the suggested controlling parameters are strongly interlinked, and the seemingly very different results obtained by researchers using different approaches are not necessarily mutually exclusive.

3. Methods

3.1. Temperature–Vegetation Dryness Index, TVDI

Following the concept in Figs. 2 and 3, isolines can be drawn in the triangle defining the T_s/NDVI space. As a first iteration to obtain information on the surface soil moisture content, a dryness index (TVDI) having the values of 1 at the "dry edge" (limited water availability) and 0 at the "wet edge" (maximum evapotranspiration and thereby unlimited water access) can be defined:

$$\mathrm{TVDI} = \frac{T_s - T_{s_{min}}}{a + b\mathrm{NDVI} - T_{s_{min}}} \quad (1)$$

where $T_{s_{min}}$ is the minimum surface temperature in the triangle, defining the wet edge, T_s is the observed surface temperature at the given pixel, NDVI is the observed normalised difference vegetation index, and a and b are parameters defining the dry edge modelled as a linear fit to data ($T_{s_{max}} = a + b\mathrm{NDVI}$), where $T_{s_{max}}$ is the maximum surface temperature observation for a given NDVI. The parameters a

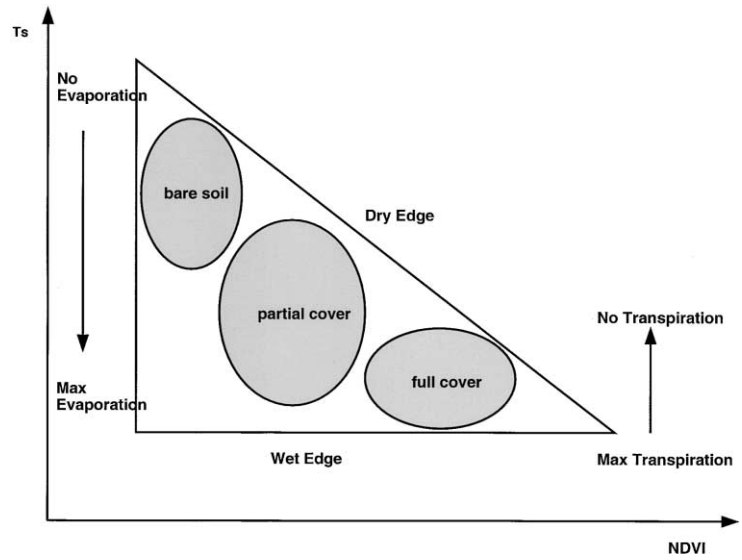

Fig. 2. Simplified T_s/NDVI (after Lambin & Ehrlich, 1996).

and b are estimated on the basis of pixels from an area large enough to represent the entire range of surface moisture contents, from wet to dry, and from bare soil to fully vegetated surfaces. The uncertainty of TVDI is larger for high NDVI values, where the TVDI isolines are closely set. The simplification of representing the T_s/NDVI space with a triangle in contrast to a trapezoid (e.g., Moran et al., 1994) adds uncertainty to TVDI at high NDVI values. Likewise, the "wet edge" is modelled as a horizontal line as opposed to a sloping wet edge in the trapezoid approach, which may lead to an over estimation of TVDI at low NDVI values.

The isolines of TVDI correspond to the temperature–vegetation index (TVX) proposed by Prihodko and Goward (1997), who estimated TVX as a bulk slope in the T_s/NDVI space for a homogeneous area (13×13 NOAA-AVHRR pixels), with little or no variation in surface moisture conditions. The T_s/NDVI space emerges when the study area is increased and variability in surface moisture conditions introduced, in other words, the TVDI isolines can be regarded as several superimposed TVX lines. Studies of T_s/NDVI slopes report steeper slopes for dryer conditions (e.g., Goetz, 1997; Nemani et al., 1993), which is in accordance with TVDI (see Fig. 3). The approach taken by several studies of the slope of T_s vs. NDVI, are thus in agreement with the concept behind TVDI, however, since TVDI may be estimated for each pixel, the full spatial

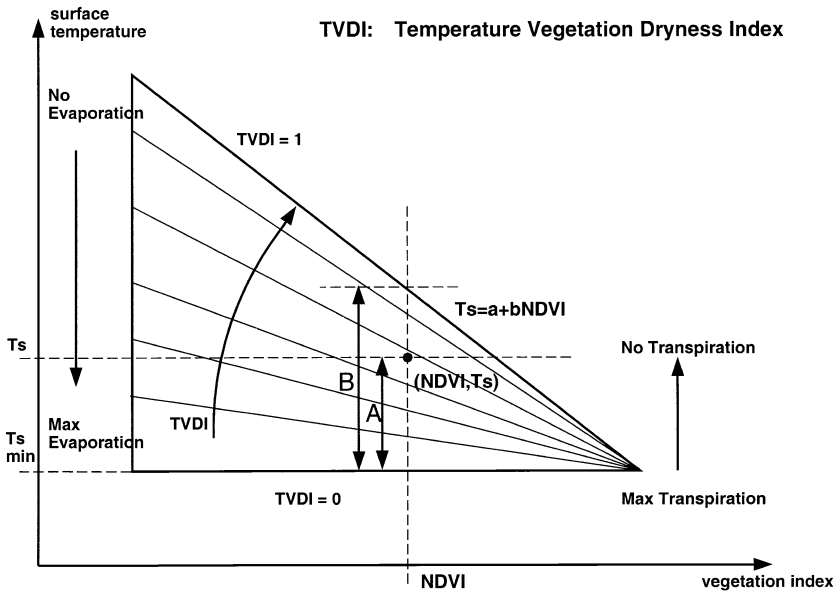

Fig. 3. Definition of the TVDI. TVDI for a given pixel (NDVI/T_s) is estimated as the proportion between lines A and B (see Eq. (1)).

resolution of data is maintained. In contrast TVX can only be computed for an area large enough to allow determination of the slope in T_s/NDVI space (i.e., contextual).

The advantage of the TVX and TVDI methods outlined here, or an approach estimating the vertices of the T_s/NDVI space empirically (e.g., Clarke, 1997), are their complete independence of ancillary data. Other approaches (e.g., Moran et al., 1994), require detailed information on the meteorological conditions, including vapour pressure deficit, wind speed, and aerodynamic resistance, to define the limits of the T_s/NDVI space. A simpler empirical estimation of the T_s/NDVI space implicitly takes these parameters into account. The approach, however, requires a large number of remotely sensed observations to ensure that the boundaries of the space are established.

3.2. Assumptions and sources of error

The empirical estimation of TVDI is based on assumptions that: (i) soil moisture is the main source of variation for T_s and (ii) TVDI is related to surface soil moisture due to changes in thermal inertia and evaporative control (evaporation and transpiration) on net radiation partitioning (energy balance).

For the operational estimation of TVDI from satellite data, a number of error sources exist: (i) no account of view angle effects on T_s and NDVI, which affects the fraction of bare soil and vegetation visible to the sensor; (ii) the "triangle" may not be determined correctly from the EO data, if the area of interest does not include a full range of variability in land surface conditions (e.g., dry bare soil, saturated bare soil, water stressed vegetation and well-watered vegetation); (iii) no account of errors in estimation of T_s (unknown and varying land surface emissivity and atmospheric effects); (iv) no account of clouds, shadows, and associated variation in net radiation; (v) decoupling of the top surface soil layer from lower layers (Capehart & Carlson, 1997); (vi) dependence of T_s and NDVI on surface type due to differences in aerodynamic resistance (Friedl & Davis, 1994; Lambin & Ehrlich, 1995).

3.3. Model simulations of soil moisture

Surface soil moisture content is not well defined over large areas, which makes validation of TVDI using surface observations difficult. In order to compare the performance of TVDI to soil moisture, a hydrological model (MIKE SHE) was used to simulate soil moisture (Andersen, Refsgaard, & Jensen, in press; Refsgaard & Storm, 1995). MIKE SHE is a development of the European Hydrological System (Systeme Hydrologique Europeen, SHE, Abbott, Bathurst, Cunge, & J., 1986). The model version used in this study is oriented towards surface water studies, so that detailed description of groundwater conditions is not required. The model is fully distributed and physically based except for the groundwater module that is only semidistributed. The model solves for interception, evapotranspiration, overland flow, channel flow, unsaturated flow, and routing of saturated subsurface flow. In this way, the major flow processes of the entire land phase of the hydrological cycle are described. The model in its current setup has been tested and calibrated for the whole Senegal River basin using daily rainfall data from 112 stations and discharge from 11 gauging stations covering a 10-year period. Input to the model included maps of vegetation type, topography, river networks, soil type and depths, and time series of precipitation, potential evapotranspiration, river discharge, LAI, and root depths. Despite spatial discretisation is 4×4 km^2, the actual spatial resolution in model output is more coarse due to low spatial resolution of the input data, particularly precipitation. The application of the model in the Senegal River basin has been described in more detail in Andersen, Sandholt, Jensen, and Refsgaard (in press) and Sandholt et al. (1999).

4. Test area and data

The 140×140 km^2 study area in the northern part of Senegal (Fig. 4) includes part of the Senegal river valley as well as dry savanna on sandy soil. The area is generally flat, with very modest relief. Mean annual precipitation is less than 200 mm with a large north–south gradient. Local variability in rainfall is high. In general, the rainy season is short, from June to September. The land cover is mainly dry grasslands with scattered trees and bushes and smaller cultivated areas in the river valley, some of them irrigated,

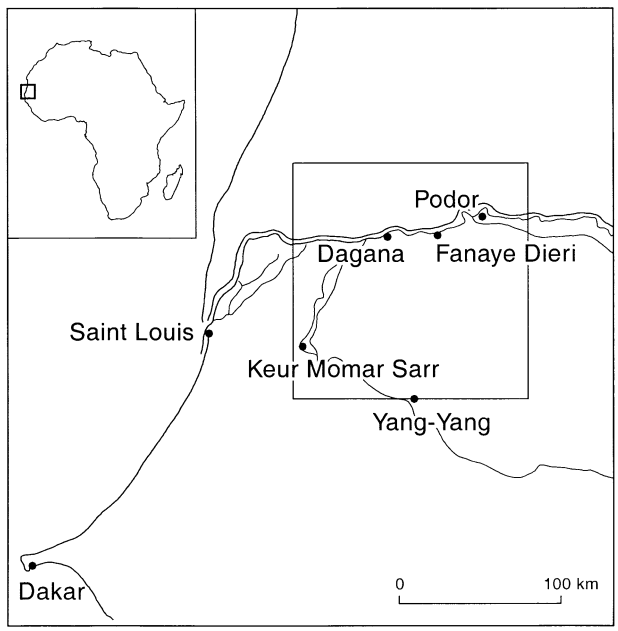

Fig. 4. The Podor subset in the northern part of Senegal. The subset is 140×140 km^2. Locations of rain gauge stations are indicated.

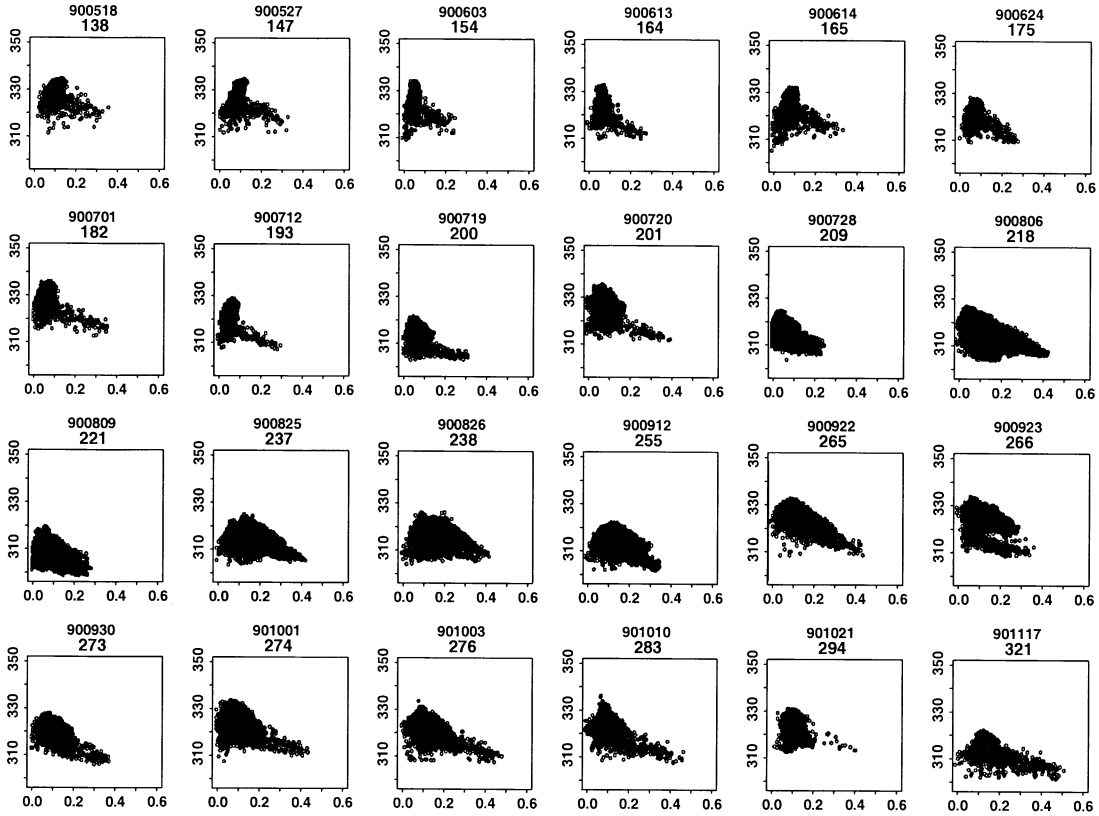

Fig. 5. Scatterplots of NDVI (x-axis) and T_s (y-axis) for the 24 images used in the study.

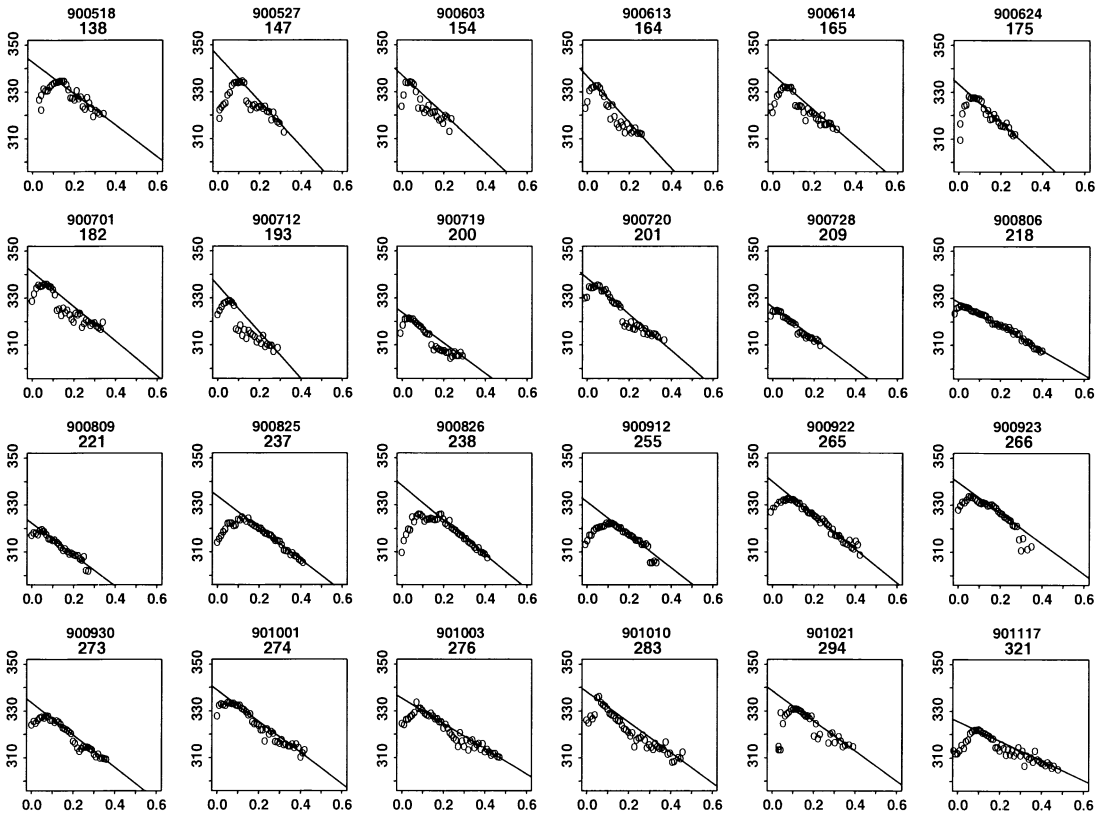

Fig. 6. Dry edge values used for estimation of TVDI. Maximum T_s was extracted for small intervals of NDVI, and the dry edge is estimated by linear regression.

others cultivated only after natural flooding. The area encompasses a range of conditions from dry bare soil in the north to wet bare soil in the river areas. The fractional vegetation cover varies over time and space. Except for irrigated fields, the study area belongs to the *water-limited group* in the T_s/NDVI space as defined by Nemani and Running (1997), where the LAI (and thus NDVI) is limited by water availability.

Of the original 74 NOAA-AVHRR images from 1990, 37 were applied in the analyses that follow. A cloud mask, based on simple thresholding in the visible and thermal channels, was applied to all images, leaving only cloud-free pixels for our analyses. Cloud margin and haze effects may still exist. We rejected 37 images with more than 50% cloud cover, and pixels with view angels larger than 42° were excluded from the analysis. The images were geometrically rectified and resampled to a pixel size of 1×1 km^2, with an accuracy less than 1 pixel. Surface temperature was calculated using a split window algorithm (Price, 1984). No atmospheric correction was performed on the visible and near infrared channels, yet atmospheric effects were minimised by use of the NDVI (Holben, 1986). All image processing was done using the NOAA application module of the CHIPS image processing system (Hansen, 1999). Precipitation data from five stations in the area were used for reference.

5. Results

5.1. T_s/NDVI space

Plots of T_s as a function of NDVI for each image (Fig. 5) showed that in 13 cases out of the 37, the range of T_s/NDVI variability was insufficient to determine the TVDI parameters. The data set was thus reduced to 24 images accounting for partial cloud cover. The dry season was characterised by low NDVI values, except for the irrigated areas in the river valley (Days 138–193 in Fig. 5). After the first rain, the variation in NDVI became larger and the T_s/NDVI range was more clearly defined (Day 200 and onwards). Later, in the rainy season, the range for some acquisitions was low again (for instance, Days 221, 266, and 294).

In order to determine the parameters describing the "dry edge," the maximum temperature observed for small intervals of NDVI was extracted in the T_s/NDVI space (Fig. 6), and the parameters were found using least squares linear regression on the sloping side of the upper edge. The concave shape of the triangles, especially in the dry season, was a result of missing data, which occurred when the natural vegetation was least extensive, i.e., when the only vegetated areas were found close to the rivers, lakes, and irrigated fields. When the middle third of the observations

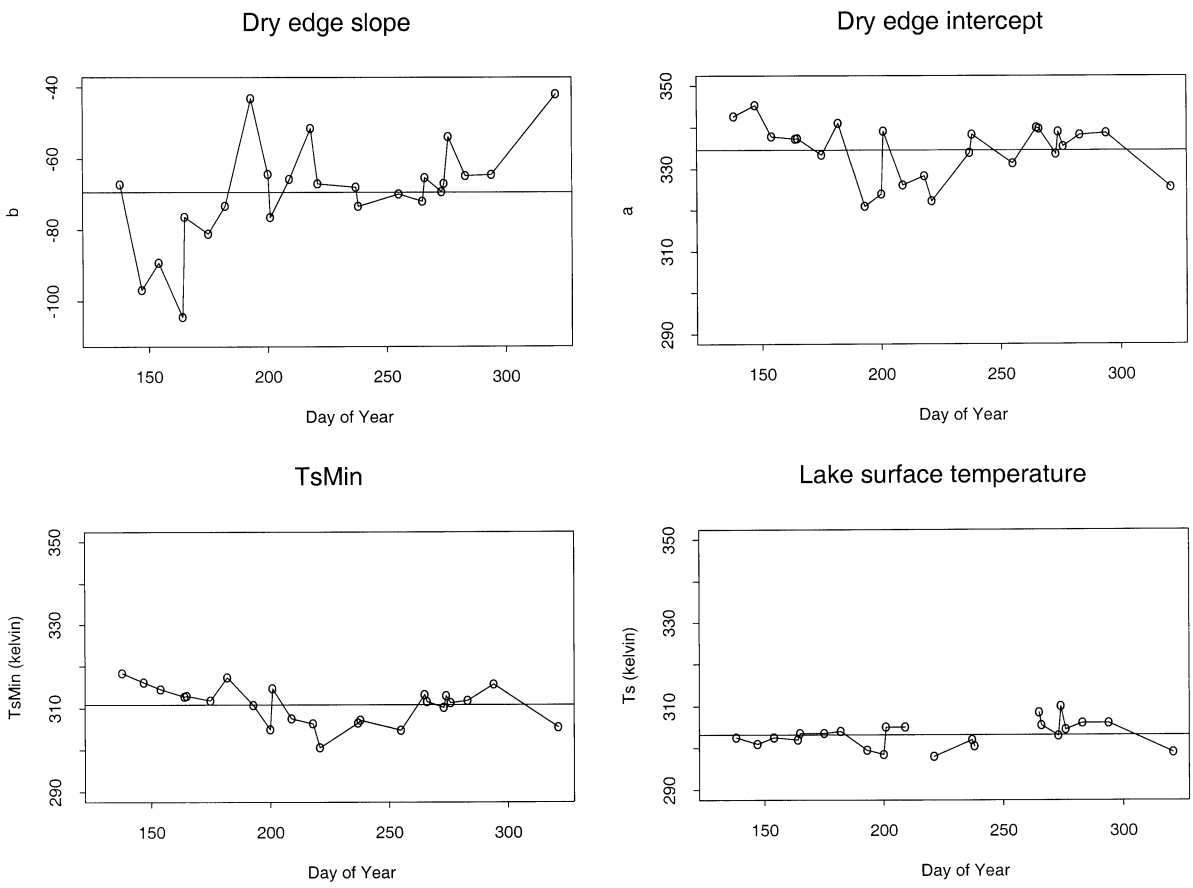

Fig. 7. Temporal evolution in TVDI parameters. Mean values are shown. Surface temperature of a large lake in the area is shown for reference.

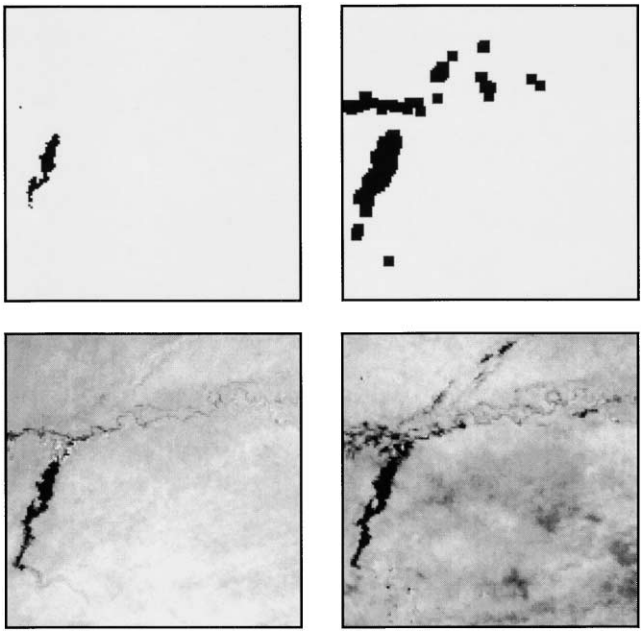

Fig. 8. TVDI for 2 days. Left: June 14 (Day 165, 1% cloud cover), right: October 21 (Day 294, 29% cloud cover). The upper row of images shows the areas masked due to clouds or lake, the lower images are TVDI maps. Bright areas correspond to dry conditions (high TVDI) and darker areas correspond to moister conditions (low TVDI).

was omitted, the extracted dry edges were better defined and the regression fits (Fig. 6) were improved. The minimum temperature in Eq. (1), estimated as the mean minimum temperature for the NDVI intervals, included areas only partly covered with vegetation, so soil surfaces had an influence on the measured brightness temperature.

TVDI parameters for the 24 images plotted as a function of time (Fig. 7) include temperature of a large lake in the area. Apparent random variation is evident in the temporal evolution of the TVDI parameters, especially in the dry season (Days 138–195) where the NDVI/T_s space is not as well defined. The slope parameter (b) stabilises around a mean value (-69) in the rainy season. No significant correlation was found between the individual TVDI parameters, lake temperature, the $T_{s_{min}}$ parameter, or the intercept. The lack of correlation and distinct trends in the parameters may be due to several factors, including highly variable atmospheric forcing. Other studies report similar behaviour of the temporal variation in slope (e.g., Goetz, 1997; Prihodko & Goward, 1997).

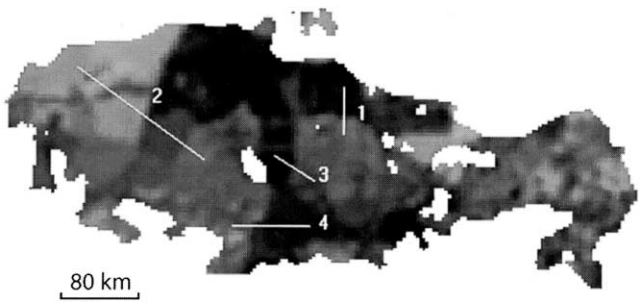

Fig. 9. Soil moisture content in the root zone as simulated with the MIKE SHE code in the northern part of the Senegal River basin, September 22, 1990. The scale has been inverted to facilitate comparison with TVDI in Fig. 10, and contrast stretched, so that dark areas correspond to moist areas, and bright areas correspond to dry areas. The four transects used for comparison with TVDI are indicated on the map (white lines, 1–4).

Fig. 10. TVDI for the same area and date as in Fig. 9. Dark areas correspond to low values of TVDI (moist areas) and bright areas correspond to high values of TVDI (dry areas).

In order to test the radiative control of surface temperature, scatter plots of surface temperature and albedo were produced for areas with low NDVI values representing bare soil. Broadband albedo was estimated from the reflectance in AVHRR channel 1, using the approach described in Nunez, Skirving, and Viney (1987). No apparent relation was found between the two variables, suggesting that other factors (evapotranspiration, thermal properties, soil moisture) had more influence than albedo, which is in accordance with the findings of Goward, Cruickhanks, and Hope (1985).

5.2. Spatial variation of TVDI

In the TVDI maps (Fig. 8), the spatial distribution of the dryness index for June 14 and October 21 is shown. The upper images show the cloud/lake mask for each image. In the June image, TVDI in the subset is high (bright values) with a mean of .75 and little spatial variation (variance .02). Low-land areas around the river and the moist area close to the lake have low dryness indices. Just north of the lake, a large irrigated sugar cane area is visible, due to the relatively high surface temperature of the homogeneous cover type (see Section 2.1), resulting in TVDI values greater than 1. The TVDI reflects local depressions in the landscape, e.g., a fossil river valley in the south of the area had a low index corresponding to moist surface conditions. The October image is generally lower (mean TVDI .53) and has large spatial variation in TVDI (variance .04).

5.3. Comparison to simulated soil moisture

Since validation using field measurements is difficult at the scale of NOAA-AVHRR imagery, the effectiveness of the proposed methodology may best be assessed by comparison to simulated soil moisture (and evapotranspiration) over large areas. TVDI is compared model simulations of

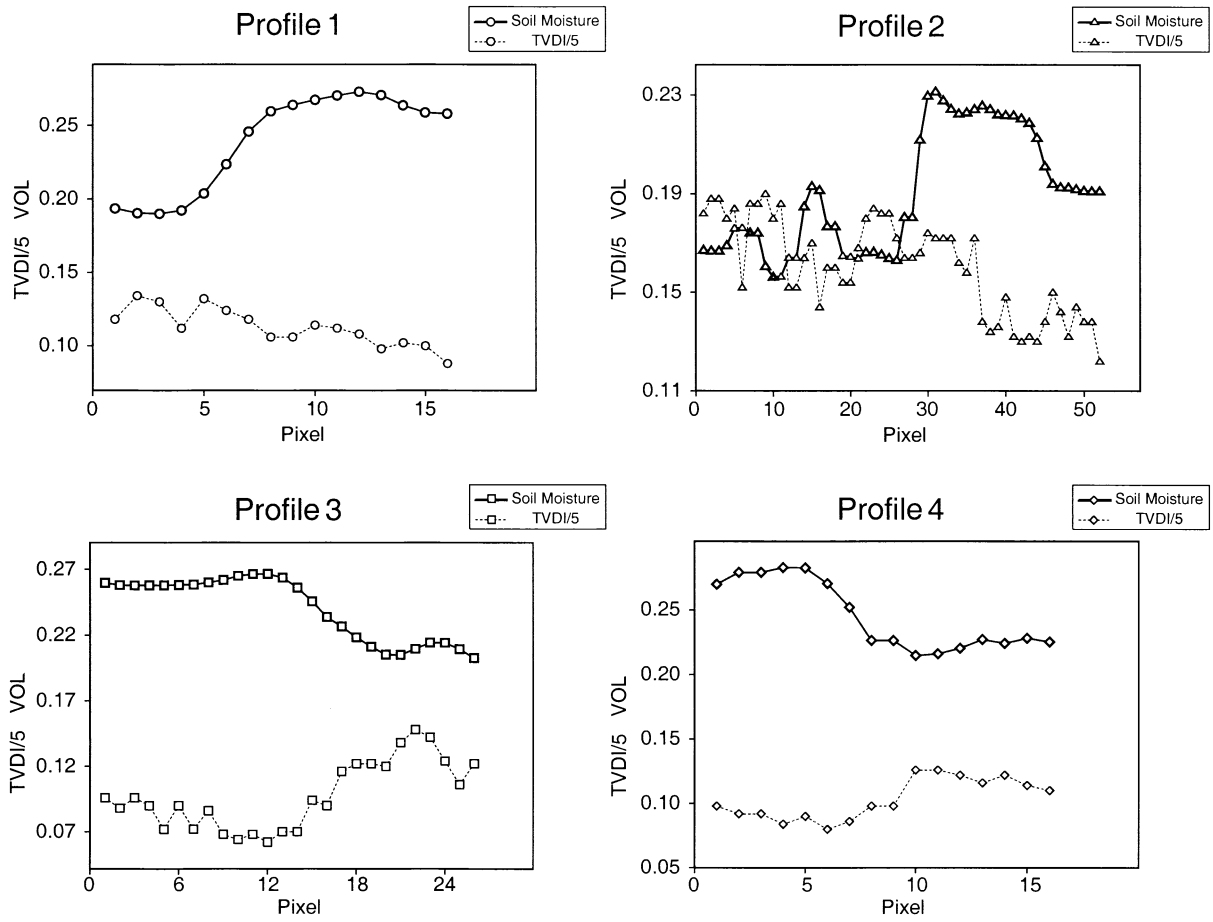

Fig. 11. TVDI values (scaled with a factor 5) as a function of simulated soil moisture along the transects indicated in Fig. 9. Each transect is approximately 80 km long except for Transect 2.

soil moisture in the root zone in the northern part of the Senegal River basin (Figs. 9 and 10). At this scale, the overall patterns found in the TVDI and simulated soil moisture images were similar, with more spatial detail in the TVDI image. The simulated soil moisture patterns were influenced by the scarcity of rain gauge measurements, the use of rain gauge data within Thiessen polygons around each rain gauge, and large spatial variability of rainfall. A detailed discussion of the hydrological model and its spatial resolution in input and output can be found in Andersen, Sandholt, et al. (2001) and Andersen, Refgaard, et al. (2000).

TVDI values for four transects drawn across areas with large and easily identifiable changes in soil moisture values (Figs. 9 and 10) mirror the soil moisture curve (Fig. 11). The poorest comparison between the two variables was for Transect 2, located in the driest area in the north of the basin.

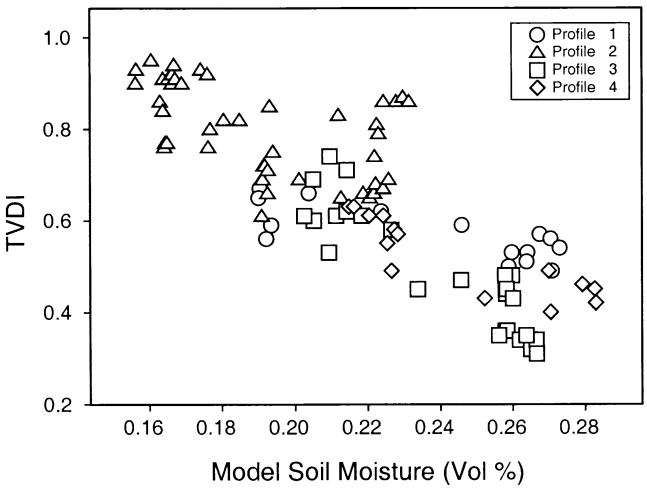

Fig. 12. Scatterplot of corresponding TVDI and soil moisture values for the four transects as indicated in Fig. 9. A linear fit to the observations has an R^2 value of .70 (Table 1).

Table 1
Mean, standard deviations of simulated soil moisture (SM) and TVDI, and R^2 values for linear fit of the data

	SM		TVDI		
Transect	Mean	S.D.	Mean	S.D.	R^2
1	.24	.03	.56	.06	.54
2	.19	.02	.80	.10	.23
3	.24	.02	.49	.13	.81
4	.25	.03	.52	.08	.70
5	.22	.04	.65	.18	.70

TVDI values plotted as a function of soil moisture (Fig. 12) show higher soil moisture values correspond to lower TVDI values and visa versa ($R^2 = .70$). Linear relationships exist between TVDI and model soil moisture with R^2 values ranging from .23 (Transect 2) to .81 (Table 1). Mean soil moisture in Transect 2 was 19%, with mean TVDI = .80, in comparison to mean TVDI values between .24 and .56 for the other transects.

5.4. Temporal evolution of TVDI

The temporal evolution of TVDI estimated for pixels representing five rain gauge stations (Fig. 4) in the 24 AVHRR images is shown in Fig. 13 together with recorded rainfall. TVDI is, in general, sensitive to rainfall, and the index drops after rain events (e.g., Day 283 for Podor, Day 274 for Dagana, and between Days 274 and 276 for Keur-Momar-Sarr). Some exceptions occur (Day 221 at Fanaye Dieri).

The overall trend in TVDI is high values in the dry season and low values in the rainy season, with greater variability in the dry season. The TVDI starts to drop below the mean dry season value with the onset of the rainy season, which is best illustrated for Dagana immediately after the first rain event (Day 182). An exception to this general trend occurs at Yang-Yang, with an unexpectedly

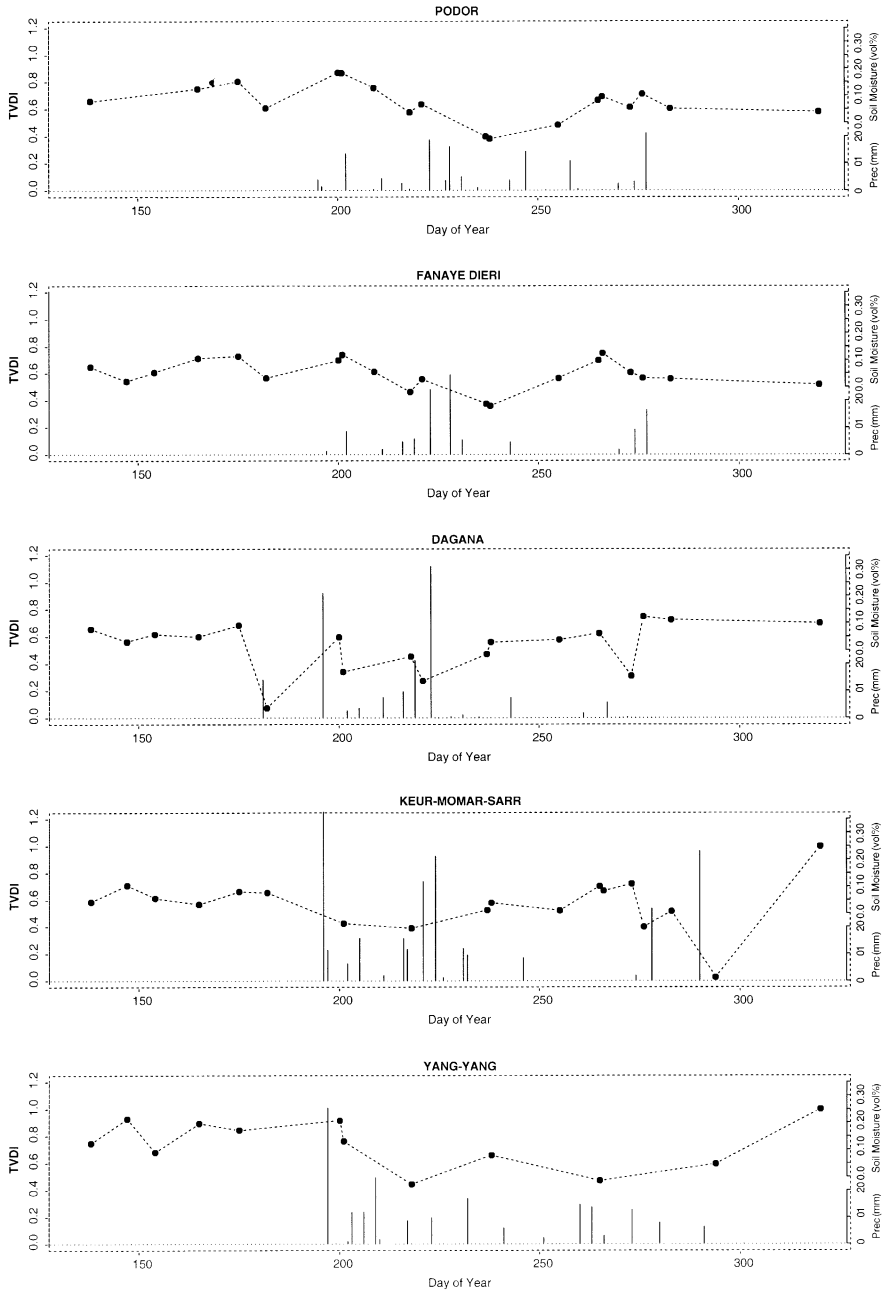

Fig. 13. TVDI plotted as a function of time. Rainfall indicated as bars.

high TVDI value on Day 200, a time of lower temperatures and lower NDVI, thus low variation in T_s/NDVI space.

Uncertainties in the estimation of the TVDI parameters has its largest impact on TVDI at higher values of NDVI. The southernmost station, Yang-Yang, which in general has higher NDVI values compared to the other stations, is located in a local depression in the landscape. A similar result was noted at Dagana (Day 200) where the rain started earlier, triggering vegetation growth.

The two uppermost graphs in Fig. 13 (Podor and Fanaye Dieri) were located 30 km apart, close to the Senegal River, thus the pattern in rainfall and TVDI curves were similar. Differences in rainfall are captured in the TVDI curves. Fanaye Dieri received no rain between Days 243 and 270, resulting in a dryer surface and higher TVDI values as compared to Podor, which had three rain events in the same period.

During the rainy season, the vegetation exploited the water in the root zone damping the TVDI, but by the end of the rainy season the TVDI values increased as the moisture status at the soil surface more than integrated values over the root zone, declined. This effect can also be seen at Dagana, where the last (minor) rain event caused the TVDI to drop, followed by a return to the dry season values.

6. Conclusion and future directions

A TVDI based on remotely sensed surface temperature and vegetation index has been suggested for use in large scale hydrological models, and tested in northern Senegal. The index is a simplification of previous formulations using only remotely sensed data. Based on the NOAA-AVHRR data used in this study, the T_s/NDVI space was well defined in most cases. Estimation of the TVDI parameters was most problematic in the dry season, and no distinct trend in the temporal evolution in the parameters was found. The TVDI technique was sensitive to cloud screening, which was in accordance with Prihodko and Goward (1997), who reported poorer T_s/NDVI air temperature estimates for areas not captured by cloud screening.

TVDI was closely related to surface soil moisture simulated with the MIKE SHE model ($R^2 = .70$). Similar spatial patterns of TVDI and simulated soil moisture were also found. Transects compared across the basin, despite different spatial resolution between the satellite and the model. A full validation of the TVDI index was not feasible in the current context, but the consistency of T_s/NDVI space and of the results from the comparison with soil moisture simulations were promising. The comparisons with model simulations demonstrate the strength of the TVDI method in the context of hydrological modelling, and the potential of using the index as an indicator of soil moisture. Still, conditions in which the methodology may be applied need to be better defined (see Goward et al., 2001). The results illustrated in Figs. 9 and 10 for the rainy season suggest an ability of the TVDI approach to provide early rainy season estimates of the spatial distribution of soil moisture in the Sahelian zone. Preliminary analyses suggest that the TVDI methodology is robust for application over larger areas, and that the shape of the T_s/NDVI space is insensitive to surface cover type, at least in semiarid West Africa (Sandholt, Rasmussen, & Andersen, in press). Additional work using meteorological data is required to test the robustness of the method over large areas, and the use of TVDI for driving, updating, and validating hydrological models.

Acknowledgments

The work was carried out as part of the project "Integration of Earth Observation Data in Distributed Agrohydrological Models" (INTEO), funded by the Danish Research Council, Grant No. 9600668. This support is greatly appreciated. Participants from the partner institutions in INTEO, the DHI Water and Environment, Department of Hydrodynamics and Water Resources (Danish Technical University), Institute of Geography (University of Copenhagen), and Centre de Suivi Ecologique, Dakar, are all acknowledged for their contributions to this work. Thanks to Centre de Suivi Ecologique, who kindly supplied the NOAA-AVHRR data. The guest editor on this special issue is acknowledged for his very useful comments during the review process, which greatly improved the paper.

References

Abbott, M., Bathurst, J., Cunge, J., & O'Connel Jr., P. E. (1986). An introduction to the European hydrological system — Systeme Hydrologique Europeen SHE 2: structure of a physically based distributed modelling system. *Journal of Hydrology*, *87*, 61–77.

Andersen, J., Refsgaard, J. C., & Jensen, K. H. (2000). Distributed hydrological modeling of the Senegal River basin — model construction and validation. *Journal of Hydrology*, (in press).

Andersen, J., Sandholt, I., Jensen, K. H., & Refsgaard, J. C. (2001). Improving the basis for validation of large scale distributed hydrological models using remotely sensed dryness index. In: M. Owe, K. Brubaker, J. Richtie, & A. Rango (Eds.), *Remote sensing and hydrology 2000, number 267 in IAHS Red Books*. Wallingford, Oxfordshire OX10 8BB, UK: IAHS/ICRS, IAHS Press, Center for Ecology and Hydrology (in press).

Boegh, E., Soegaard, H., Hanan, N., Kabat, P., & Lesch, L. (1998). A remote sensing study of the NDVI–T_s relationship and the transpiration from sparse vegetation in the Sahel based on high resolution satellite data. *Remote Sensing of Environment*, *69* (3), 224–240.

Capehart, W. J., & Carlson, T. N. (1997). Decoupling of surface and near-surface soil water content: a remote sensing perspective. *Water Resources Research*, *33* (6), 1383–1395.

Carlson, T. N., Gillies, R. R., & Perry, E. M. (1994). A method to make use of thermal infrared temperature and NDVI measurements to infer surface soil water content and fractional vegetation cover. *Remote Sensing Reviews*, *9*, 161–173.

Carlson, T. N., Gillies, R. R., & Schmugge, T. J. (1995). An interpretation

of methodologies for indirect measurement of soil water content. *Agricultural and Forest Meteorology*, *77*, 191–205.

Clarke, T. R. (1997). An empirical approach for detecting crop water stress using multispectral airborne sensors. *HortTechnology, A Publication of the American Society for Horticultural Science Alexandria, VA 2314*, *7* (1), 9–16.

Czajkowski, K. P. (2001). Thermal remote sensing of near-surface water vapor. *Remote Sensing of Environment*, *79*, 253–265.

Friedl, M. A., & Davis, F. W. (1994). Sources of variation in radiometric surface temperature over a tallgrass prairie. *Remote Sensing of Environment*, *48*, 1–17.

Gillies, R. R., Carlson, T. N., Gui, J., Kustas, W. P., & Humes, K. S. (1997). A verification of the 'triangle' method for obtaining surface soil water content and energy fluxes from remote measurements of the Normalized Difference Vegetation Index (NDVI) and surface radiant temperature. *International Journal of Remote Sensing*, *18* (15), 3145–3166.

Goetz, S. J. (1997). Multisensor analysis of NDVI, surface temperature and biophysical variables at a mixed grassland site. *International Journal of Remote Sensing*, *18* (1), 71–94.

Goward, S. N., Cruickhanks, G. D., & Hope, A. S. (1985). Observed relation between thermal emission and reflected spectral radiance of a complex vegetated landscape. *Remote Sensing of Environment*, *18*, 137–146.

Goward, S. N., Xue, Y., & Czajkowski, K. P. (2001). Evaluating land surface moisture conditions from the remotely sensed temperature/vegetation index measurements: an exploration with the simplified simple biosphere model. *Remote Sensing of Environment*, (this issue).

Hansen, L. (1999). *CHIPS for Windows, Version 4.4a. Users Guide* (1st ed.). Ostervoldgade 10, DK-1350 Copenhagen K, Denmark: CDT, Institute of Geography, University of Copenhagen.

Holben, B. (1986). Characteristics of maximum-value composite images from temporal AVHRR data. *International Journal of Remote Sensing 7*, 1417–1434.

Lambin, E. F., & Ehrlich, D. (1995). Combining vegetation indices and surface temperature for land-cover mapping at broad spatial scales. *International Journal of Remote Sensing*, *16* (3), 573–579.

Lambin, E. F., & Ehrlich, D. (1996). The surface temperature–vegetation index space for land cover and land-cover change analysis. *International Journal of Remote Sensing*, *17*, 463–487.

Moran, M. S., Clarke, T., Kustas, W. P., Weltz, M., & Amer, S. A. (1994). Evaluation of hydrologic parameters in a semiarid rangeland using remotely sensed spectral data. *Water Resources Research*, *30* (5), 1287–1297.

Moran, M. S., Clarke, T. R., Inoue, Y., & Vidal, A. (1994). Estimating crop water deficit using the relation between surface-air temperature and spectral vegetation index. *Remote Sensing of Environment*, *49*, 246–263.

Nemani, R., Pierce, L., Running, S., & Goward, S. (1993). Developing satellite-derived estimates of surface moisture status. *Journal of Applied Meteorology*, *32* (3), 548–557.

Nemani, R., & Running, S. (1997). Land cover characterization using multi-temporal red, near-IR and thermal-IR data from NOAA/AVHRR. *Ecological Applications*, *7* (1), 79–90.

Nemani, R. R., & Running, S. W. (1989). Estimation of regional surface resistance to evapotranspiration from NDVI and thermal IR AVHRR data. *Journal of Applied Meteorology*, *28*, 276–284.

Nunez, M., Skirving, J., & Viney, R. (1987). A technique for estimating regional surface albedos using geostationary satellite data. *Journal of Climatology*, *7*, 1–11.

Price, J. C. (1984). Land surface temperature measurements from the split window channels of the NOAA-7 advanced very high resolution radiometer. *Journal of Geophysical Research*, *89*, 7231–7237.

Price, J. C. (1990). Using spatial context in satellite data to infer regional scale evapotranspiration. *IEEE Transactions on Geoscience and Remote Sensing*, *28*, 940–948.

Prihodko, L., & Goward, S. N. (1997). Estimation of air temperature from remotely sensed surface observations. *Remote Sensing of Environment*, *60* (3), 335–346.

Refsgaard, J., & Storm, B. (1995). MIKE SHE. In: V. Singh (Ed.), *Computer models of watershed hydrology* (pp. 809–846). Water Resources Publication Co. USA.

Sandholt, I., Andersen, J., Dybkjaer, G., Lo, M., Rasmussen, K., Refsgaard, J. C., & Jensen, K. H. (1999). Use of remote sensing data in distributed hydrological models: applications in the Senegal River basin. *Danish Journal of Geography*, *99*, 47–57.

Sandholt, I., Rasmussen, K., & Andersen, J. (2001). Derivation of a dryness index from NOAA-AVHRR data for use in large scale hydrological modeling. In: M. Owe, K. Brubaker, J. Richtie, & A. Rango (Eds.), *Remote sensing and hydrology 2000, number 267 in IAHS Red Books*. Wallingford, Oxfordshire OX10 8BB, UK: IAHS/ICRS, IAHS Press, Centre for Ecology and Hydrology (in press).

Smith, R. C. G., & Choudhury, B. J. (1991). Analysis of normalized difference and surface temperature observations over southeastern Australia. *International Journal of Remote Sensing*, *12* (10), 2021–2044.

Troufleau, D., & Soegaard, H. (1998). Deriving surface water status in the Sahel from the Pathfinder AVHRR Land data set. *Physics and Chemistry of the Earth*, *23* (4), 421–426.

Zeng, X. B. (1999). The relationship among precipitation, cloud-top temperature, and precipitable water over the tropics. *Journal of Climate*, *12* (8), 2503–2514.